CrystEngComm

PAPER

View Article Online
View Journal | View Issue

Cite this: *CrystEngComm*, 2021, **23**, 7278

Selectivity behaviour of two roof-shaped host compounds in the presence of xylene and ethylbenzene guest mixtures†

Benita Barton, * Brandon Barnardo and Eric C. Hosten

In the present investigation, we compare the host and selectivity behaviour of two compounds, namely α,α-diphenyl-9,10-dihydro-9,10-ethanoanthracene-11-methanol **H1** and α,α-bis(*p*-chlorophenyl)-9,10-dihydro-9,10-ethanoanthracene-11-methanol **H2**, when recrystallized from both singular and mixed isomers comprising the xylenes (*o*-Xy, *m*-Xy and *p*-Xy) and ethylbenzene (EB) as potential guest solvents. **H1** formed a complex with *o*-Xy alone in the single solvent experiments, while **H2** included all four of these aromatic compounds. In equimolar guest competition experiments, **H1** only crystallized from binary mixtures where *o*-Xy was present, and high selectivities for this guest were observed in these instances (84.5–93.7%). The other binary mixtures ultimately presented as gels, and **H1** therefore failed to crystallize from these. In fact, this was true also for all ternary and quaternary experiments with **H1**, even when *o*-Xy was present. **H2**, on the other hand, consistently formed mixed complexes from all of the solutions employed. However, its selectivity for any particular guest was unremarkable. Guest/guest competition experiments using both equimolar and non-equimolar mixtures revealed that **H1** may be employed to purify *o*-Xy/*m*-Xy, *o*-Xy/*p*-Xy and *o*-Xy/EB binary mixtures, especially when these solutions comprised 50% or more *o*-Xy (these experiments all favoured *o*-Xy). SCXRD analyses were employed to understand the moderate preference of **H2** for *o*-Xy: only this guest was involved in contacts with the host compound, two in number, that measured significantly less than the sum of the van der Waals radii of the atoms involved. Additionally, Hirshfeld surface investigations showed that **H2**, through its chlorine atoms, was involved in the greater number of contacts with the preferred *o*-Xy guest compound. Thermal analyses, however, proved less useful in understanding these selectivity data.

Received 26th August 2021,
Accepted 21st September 2021

DOI: 10.1039/d1ce01149a

rsc.li/crystengcomm

1. Introduction

Very recently, there has been much interest in the field of host–guest chemistry as investigations continue in the search for efficient alternative separation or purification protocols for combinations of the xylenes and ethylbenzene.[1–3] Due to their narrow boiling range (136.2–144.5 °C) when crude oil is distilled, these isomeric compounds distil across more or less simultaneously and are thus isolated as a mixture. Further tedious, costly and energy-intensive fractional distillations/crystallizations are then warranted in order to obtain each component in pure form and, oftentimes, these processes may not be effective enough to afford these compounds with optimal purities for further synthetic applications.[4] As an example, *p*-xylene is a tremendously important building block towards polyethylene terephthalate (PET), accepted as the most important commercial polyester polymer. The process involves, first, the oxidation of *p*-xylene to form terephthalic acid which then undergoes an esterification reaction to furnish dimethyl terephthalate (DMT). In order for the polymerization of DMT to PET to be successful, it is required that DMT be extremely pure,[5] and this requisite is made all the more difficult to attain if the starting xylene lacked in adequate purity. Hence there exists a need for more efficient, less energy-consuming and lower cost separatory techniques, and host–guest chemistry presents itself as one such alternative protocol. Besides the relatively simple syntheses of the host compounds in most cases, this field of chemistry is a very attractive substitute given the facile recyclability of the host material in such applications, which has a direct

Department of Chemistry, Nelson Mandela University, PO Box 77000, Port Elizabeth, 6031, South Africa. E-mail: benita.barton@mandela.ac.za

† Electronic supplementary information (ESI) available: Fig. S1a–c (**H1**) and S2a–f (**H2**) (ESI) are the selectivity profiles that were obtained after plotting *Z* (the mole ratio of G_A or G_B in the host crystals) against *X* (the mole ratio of the same guest in the solution). Fig. S3a–e are the overlaid DSC, TG and DTG traces for **H1**·*o*-Xy, **H2**·*o*-Xy, **H2**·*m*-Xy, **H2**·*p*-Xy and **H2**·EB, respectively. CCDC numbers 2088997 (**H1**·*o*-Xy), 2088998 (**H2**·*o*-Xy), 2088999 (**H2**·*m*-Xy), 2089000 (**H2**·*p*-Xy) and 2089001 (**H2**·EB). For ESI and crystallographic data in CIF or other electronic format see DOI: 10.1039/d1ce01149a

consequence on the overall cost of the process and the rampant depletion of fossil fuels.

In our laboratories, we have spent much time and resources on this very challenge by preparing host compounds derived from tartaric acid, xanthone and thioxanthone, and presenting these with various mixtures of the xylene and ethylbenzene isomers (*o*-Xy, *m*-Xy, *p*-Xy and EB).[6–11] Excellent selectivities (95–97%) were observed for *p*-Xy when the host compounds were *N*,*N*′-bis(9-phenyl-9-xanthenyl)ethylenediamine[7] and *N*,*N*′-bis(9-phenyl-9-thioxanthenyl)ethylenediamine,[8] alluding to the possibility of employing these host compounds for successful separations of certain mixtures of these isomers. Several other researchers have also focussed their energies on this industrial problem, and reports by Wicht[3] and Nassimbeni *et al.*[12] serve as fitting examples thereof. An exciting article by Day *et al.*[13] investigated both perethylated pillar[5]- and pillar[6]-arenes (EtP5 and EtP6) for this function and found that the latter arene performed extremely well, separating the *para*- from the *meta*- and *ortho*-isomers with 90% specificity. Single crystal diffraction analyses revealed the *para*-xylene molecule to be located almost exactly in the middle of the cavity of EtP6. There have, furthermore, been numerous reports detailing the employment of metal- and covalent-organic frameworks (MOFs and COFs), as well as zeolites, for the separation of these aromatic C_8H_{10} isomers.[14–16]

Notwithstanding the myriad reports dealing with the separation of Xy/EB mixtures, the quest for different host compounds with greater advantages relative to known contenders in these guest/guest competition conditions remains ongoing. Host compounds that present fewer complications with respect to their syntheses and yields, that are obtainable readily and at low cost, and that have enhanced selectivities for one or another of these guest components, are constantly being sought. To this end, we have recently embarked upon assessing the roof-shaped host compounds, the brainchild of Prof Edwin Weber,[17] for their adeptness as separation or purification tools for Xy/EB mixtures. The roof-shaped host compound *trans*-9,10-dihydro-9,10-ethanoanthracene-11,12-dicarboxylic acid displayed remarkable selectivity for *p*-Xy (94–97%) when the other guest present was either *o*-Xy or *m*-Xy, even when the concentration of *p*-Xy in solution was as low as approximately 30%.[18] Its dimethyl ester, however, performed poorly in analogous conditions. In a similar fashion, competition experiments employing *trans*-α,α,α′,α′-tetraphenyl-9,10-dihydro-9,10-ethanoanthracene-11,12-dimethanol and *trans*-α,α,α′,α′-tetra(*p*-chlorophenyl)-9,10-dihydro-9,10-ethanoanthracene-11,12-dimethanol showed the latter to be significantly more selective than the former, and the selectivity for *m*-Xy from *o*-Xy/*m*-Xy mixtures exceeded 91%.[19] The behaviour of the former unsubstituted phenyl derivative was only ordinary in most of the recrystallization experiments conducted in that work.

In the current investigation, we report on the behaviour of related roof-shaped host compounds α,α-diphenyl-9,10-dihydro-9,10-ethanoanthracene-11-methanol **H1** and α,α-bis(*p*-chlorophenyl)-9,10-dihydro-9,10-ethanoanthracene-11-methanol **H2** when these were recrystallized from various mixtures containing Xy/EB (Scheme 1). While Weber *et al.*[17] briefly mentioned that the selectivity of **H1** was for *o*-Xy when presented with binary *o*-Xy/benzene, *o*-Xy/toluene, *o*-Xy/*m*-Xy and *o*-Xy/*p*-Xy solutions, no further guest/guest competitions were carried out with this host compound in that or any other reports from the literature. Similarly, the literature contains no record of similar experiments with **H2**. Only two reports were uncovered that noted the single solvent inclusion complexes formed by **H1** with acetone and toluene,[20] and by **H2** with cyclohexylamine and ethyl acetate,[21] but no further investigations were conducted. We report here on all selectivity data obtained after analyses of solids emanating from the recrystallization experiments of **H1** and **H2** from these Xy/EB mixtures. Additionally, this report provides information from single crystal diffraction analyses, where five novel crystal structures are elucidated, as well as the results obtained from thermoanalytical experiments on these complexes.

2. Experimental

2.1 General

All chemicals and solvents were purchased from Sigma-Aldrich in South Africa and used without further modification. ^{1}H-NMR experiments were conducted on a Bruker Ultrashield Plus 400 MHz spectrometer. GC-MS analyses were carried out using a Young Lin YL6500 gas chromatograph coupled to a flame ionization detector, and dichloromethane was the dissolution solvent for the complexes of both host compounds. For the xylenes and ethylbenzene guest solvents, an Agilent J&W Cyclosil-B column was applicable. The method involved an initial 1 min hold time at 50 °C followed by a ramp of 10 °C min^{-1} until 90 °C was reached. This temperature was maintained for 3 min during which time the last peak eluted from the column. The flow rate was 1.5 mL min^{-1} with a split ratio of 1 : 80. Due to instrument availability, an Agilent 7890A gas chromatograph coupled to an Agilent 5975C VL spectrometer was also used at times; the column remained the same. Again, the method involved an initial hold time of 1 min at 50 °C after which the sample was heated at 0.5 °C min^{-1} until 52 °C was reached, and then at 0.3 °C min^{-1} until it reached a temperature of 54 °C. The flow rate was, again, 1.5 mL min^{-1} and the split ratio 1 : 100.

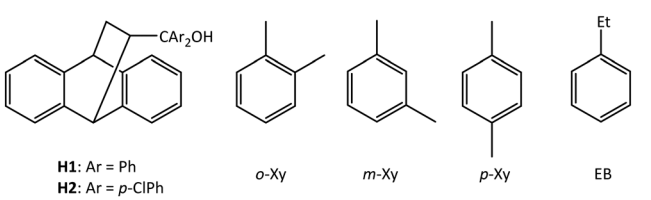

Scheme 1 Structures of roof-shaped host compounds **H1** and **H2**, and the potential xylene and ethylbenzene guest isomers.

2.2 Synthesis of the roof-shaped host compounds H1 and H2

Both roof-shaped host compounds (**H1** and **H2**) were readily synthesized in good yield by considering the methods of Weber *et al.*[17]

2.3 Recrystallization experiments of the host compounds from singular solvents

In order to determine whether **H1** and **H2** are efficient host compounds for *o*-Xy, *m*-Xy, *p*-Xy and EB, each one was recrystallized independently from the four organic solvents. To achieve this, **H1** or **H2** (0.05 g) was dissolved in an excess of each of these guests (6–7 mmol) in glass vials. The vials were then left open to the ambient conditions which facilitated crystallisation. The crystals were collected under suction and washed with low boiling petroleum ether (40–60 °C). Analysis of these solids was by means of ^{1}H-NMR spectroscopy. The host : guest ratios (H : G) of successfully-formed complexes were calculated by comparing the areas under the peaks for selected host and guest resonance signals.

2.4 Recrystallization experiments of the host compounds from equimolar mixed guests

To investigate the selectivities of **H1** and **H2** for any of the guest components, each host compound was recrystallized from binary, ternary and quaternary mixtures of these guests where each guest was present in equimolar amounts. Therefore **H1** or **H2** (approximately 0.05 g) was dissolved in the guest mixture (7 mmol combined amount), and the vials closed and stored in a refrigerator (0 °C). Any crystals that formed in this way were again collected under suction, washed with petroleum ether and analysed by means of GC-MS. These analyses provided the G : G ratios of each of the mixed complexes (as appropriate) while ^{1}H-NMR spectroscopy was employed to determine the overall H : G ratios.

2.5 Recrystallization experiments of the host compounds from binary guest mixtures in varying proportions

The selectivity behaviour of each host compound was also assessed in binary guest mixtures where the concentration of each guest component present was varied. The guest molar ratios thus employed approximated 80 : 20, 60 : 40, 50 : 50, 40 : 60 and 20 : 80 for guests A (G_A) and B (G_B), respectively. Thus, after mixing the solvents in these proportions, each host compound (0.05 g) was dissolved in the resultant solution (the combined guest amount remained 7 mmol), and the vials treated in the same manner as in the equimolar experiments. Both phases were analysed by GC-MS, the solution (*X*) as well as the crystals emanating from the solution (*Z*). Therefore, these analyses provided the $G_A : G_B$ ratios in each of the phases, and a plot of *Z* for G_A (or G_B) against *X* for G_A (or G_B) afforded selectivity profiles which depict the selectivity behaviour of the host compound in such varying conditions.[22] The selectivity coefficient, $K_{G_A:G_B}$, obtained using the equation $K_{G_A:G_B} = Z_{G_A}/Z_{G_B} \times X_{G_B}/X_{G_A}$, where $X_{G_A} + X_{G_B} = 1$, measures the host selectivity. Fig. S1a–c and S2a–f (ESI†) were the result of these plots, wherein have been inserted straight lines to demonstrate the behaviour of an unselective host compound (where $K = 1$) compared with the experimental data points.

2.6 Single crystal X-ray diffraction (SCXRD) analyses

SCXRD experiments were conducted at 200 or 296 K using a Bruker Kappa Apex II diffractometer with graphite-monochromated Mo Kα radiation (λ = 0.71073 Å). APEXII was used for data collection while SAINT was employed for cell refinement and data reduction.[23] SHELXT-2018/2[24] was utilized to solve the structures, and these were refined by means of least-squares procedures using SHELXL-2018/3[25] together with SHELXLE[26] as a graphical interface. All non-hydrogen atoms were refined anisotropically. Carbon-bound hydrogen atoms were added in idealised geometrical positions in a riding model. The hydrogen atoms of the hydroxyl groups were allowed to rotate with a fixed angle around the C–O bond to best fit the experimental electron density. Data were corrected for absorption effects using the numerical method implemented in SADABS.[23] *o*-Xy and *m*-Xy in crystals of **H2** were disordered and required the use of various constraints and restraints. The new crystallographic data for the five complexes produced in this work were deposited at the Cambridge Crystallographic Data Centre (CCDC), with CCDC numbers 2088997 (**H1**·*o*-Xy), 2088998 (**H2**·*o*-Xy), 2088999 (**H2**·*m*-Xy), 2089000 (**H2**·*p*-Xy) and 2089001 (**H2**·EB).

2.7 Thermal analyses

Successfully-formed complexes arising from recrystallization experiments of the host compounds from singular guest solvents were analysed by means of thermoanalytical experiments (these solids were recovered as usual and were not further manipulated). The thermal experiments were performed by means of a TA SDT Q600 Module system while resultant data were analysed using TA Universal Analysis 2000 software. Samples were placed in open platinum pans, and an empty pan functioned as the reference. The purge gas was high purity nitrogen. Samples were heated from approximately 40 to 400 °C, and the heating rate was 10 °C min^{-1}. Dependent on instrument availability, some of these analyses were performed using a Perkin Elmer STA6000 simultaneous thermal analyser and analysed using Perkin Elmer Pyris 13 thermal analysis software. In this instance, an empty ceramic pan was used for both the reference and then the sample run.

3. Results and discussion

3.1 Recrystallization experiments of the host compounds from singular solvents

The ^{1}H-NMR results obtained after isolating and analysing the crystals emanating from the recrystallization experiments of **H1** and **H2** from each of the xylenes and EB are summarized in Table 1. Interestingly, **H1** was significantly more selective in its behaviour compared with **H2**, enclathrating only *o*-Xy; in

Table 1 H : G ratios of complexes formed upon recrystallization of compounds **H1** and **H2** from the xylenes and EB[a]

Guest	**H1** : G ratio	**H2** : G ratio
o-Xy	1 : 1	1 : 1
m-Xy	[b]	1 : 1
p-Xy	[b]	1 : 1
EB	[b]	1 : 1

[a] The H : G ratios were obtained from ^{1}H-NMR spectra of the resultant crystals from each recrystallization experiment. [b] The guest was not enclathrated and only apohost crystallized from these solutions.

experiments with *m*-Xy, *p*-Xy and EB, only apohost host **H1** crystallized from the solutions. The *p*-chloro host derivative **H2**, on the other hand, formed complexes with each of the four isomers. In all successful complexation experiments, the preferred H : G ratio remained 1 : 1.

3.2 Recrystallization experiments of the host compounds from equimolar mixed guests

Table 2 summarizes the GC-MS (for G : G ratios) and ^{1}H-NMR (for overall H : G ratios) data obtained upon recrystallizing each of the host compounds from mixtures comprising equimolar amounts of every possible binary, ternary and quaternary combination of the four guest isomers. These experiments were conducted in duplicate, and this table contains the averaged values. Percentage e.s.d.s are, furthermore, provided in parentheses.

Remarkably, **H1** only crystallized out in binary mixtures that contained *o*-Xy. The other binary guest combinations afforded only gels (no crystallization was observed in these instances). In fact, all other experiments involving **H1** failed to afford any crystals at all, even the ternary and quaternary solutions in which *o*-Xy was present. Notably, the preference for *o*-Xy in the successful recrystallizations was significant (84.5–93.7%) and, considering that only *o*-Xy formed a complex with **H1** in the single solvent experiments (Table 1), this selectivity behaviour was somewhat anticipated. However, what was not predicted was the poor crystallinity of this host compound in the absence of *o*-Xy in the remaining binary guest combinations and in any ternary or higher combinations of these organic solvents, even where *o*-Xy was present. Ultimately, however, it may be concluded that **H1** would serve as a highly efficient host compound for the purification of *o*-Xy in binary mixtures where the other guest is either *m*-Xy, *p*-Xy or EB and, more especially, in the latter case, by employing host–guest chemistry protocols.

In comparison to **H1**, host compound **H2** was only moderate in its selectivity behaviour when recrystallized from these mixed guests. Optimal results were obtained in the binary experiments in which *o*-Xy was present, with some preference being noted for this guest compound (66.8–74.6%). In the absence of *o*-Xy, the *meta* isomer was favoured in *m*-Xy/*p*-Xy (61.7%), and *p*-Xy in *p*-Xy/EB (71.8%), while the *m*-Xy/EB experiment afforded crystals only slightly enriched with *m*-Xy (53.3%). Finally, all of the ternary experiments resulted in mixed complexes where the host selectivity behaviour was poor (40.1–54.9%). Interestingly, the data obtained from a number of different quaternary mixture experiments revealed the host selectivity to be inconsistent in both its preferred guest species and also the extent of its selectivity. These data were thus not provided here. Overall, then, this host compound would thus not be suitable for the efficient purification of any of these combinations of solvents.

3.3 Recrystallization experiments of the host compounds from binary guest mixtures in varying proportions

Fig. S1a–c (**H1**) and S2a–f (**H2**) (ESI†) are the selectivity profiles that were obtained after plotting *Z* (the mole ratio of G_A or G_B in the host crystals) against *X* (the mole ratio of the same guest in the solution).

Table 2 Mixed complexes formed by **H1** and **H2** after recrystallization from the various equimolar solutions of the xylenes and EB[a,b]

				H1	**H2**
o-Xy	*m*-Xy	*p*-Xy	EB	G : G ratios (% e.s.d.s)	G : G ratios (% e.s.d.s)
X	X			**87.3** : 12.7 (0.7)	**66.8** : 33.2 (1.2)
X		X		**84.5** : 15.5 (0.1)	**73.9** : 26.1 (1.6)
X			X	**93.7** : 6.3 (0.5)	**74.6** : 25.4 (1.9)
	X	X		[c]	**61.7** : 38.3 (1.4)
	X		X	[c]	**53.3** : 46.7 (1.0)
		X	X	[c]	**71.8** : 28.2 (1.0)
X	**X**	X		[c]	38.4 : **40.1** : 21.5 (0.9 : 0.4 : 1.1)
X	X		**X**	[c]	1.7 : 48.4 : **49.9** (0.2 : 0.9 : 0.7)
X		X	X	[c]	**54.9** : 22.8 : 22.3 (1.0 : 0.5 : 1.4)
	X	X	X	[c]	**50.0** : 30.6 : 19.4 (1.3 : 0.4 : 1.8)
X	X	X	X	[c]	[d]

[a] The data contained herein were obtained from GC-MS analyses and are the averages of two analogous experiments; % e.s.d.s are thus provided in parentheses. [b] In all cases where complexation was successful, the overall H : G ratio, obtained from ^{1}H-NMR spectroscopy, was consistently 1 : 1. [c] Crystallization did not occur, and a gel remained in the vessel. [d] The results obtained from many different quaternary mixture experiments and **H2** afforded mixed complexes in which both the preferred guest species and the extent of selectivity were inconsistent and thus unreliable.

The three profiles obtained for **H1**, *o*-Xy/*m*-Xy (Fig. S1a†), *o*-Xy/*p*-Xy (Fig. S1b†) and *o*-Xy/EB (Fig. S1c†), showed that mixed complexes were formed in each instance and that most of these were all considerably enriched with *o*-Xy (note that none of the other binary experiments afforded crystals, and gels remained behind in the glass vessels). These results are not surprising given that only *o*-Xy was enclathrated by **H1** in the single solvent experiments (Table 1). The averaged *K* values were determined to be 4.9, 6.0 and 5.0, respectively. From Fig. S1a,† it is feasible to propose **H1** as a host candidate for the purification of mixtures of *o*-Xy and *m*-Xy where the former is present in quantities close to and greater than 50% while, similarly, *o*-Xy/*p*-Xy mixtures (Fig. S1b†) may be purified when the molar ratio of *o*-Xy is between 60 and 80% of the solution. In all these aforementioned experiments, the crystals that resulted contained almost 90% or more *o*-Xy. The *o*-Xy/EB experiment (Fig. S1c†), however, differed somewhat in that only the 50 : 50 mixture produced crystals with significantly enhanced quantities of *o*-Xy. The experiment was repeated thrice in order to ensure that this result was not an outlier and, each time, the resultant crystals contained close to 95% *o*-Xy. In fact, the *K* value at this point was, satisfyingly, 13.8, indicative that **H1** may be employed successfully to separate such mixtures. Otherwise, in the case of this profile, the behaviour of **H1** appeared rather unpredictable, especially when the solution contained just over 40% *o*-Xy. Once more, this experiment was repeated with very little change in the observed result.

In the binary experiments with **H2**, the host selectivity was much reduced in each case relative to analogous experiments with **H1**. Only in three of these profiles was it observed that **H2** preferred only one guest, namely in the *o*-Xy/*m*-Xy (Fig. S2a†), *o*-Xy/EB (Fig. S2c†) and *p*-Xy/EB (Fig. S2f†) solutions, where *o*-Xy, *o*-Xy and *p*-Xy were favoured, respectively. Averaged *K* values were, however, low (1.6–2.4). In the remaining three experiments (Fig. S2b, S2d and S2e†), the behaviour of **H2** was dependent on the guest concentrations in the solutions and all calculated *K* values were unremarkable (1.9–3.2).

To conclude, the preferential behaviour of **H1** in the binary solutions was considerably enhanced and always in favour of *o*-Xy, alluding to the possibility that this host compound may be employed to purify these mixtures. This is especially the case when these solutions contained more of the *o*-Xy guest species in the case of *o*-Xy/*m*-Xy and *o*-Xy/*p*-Xy mixtures, or exactly 50% *o*-Xy in the case of *o*-Xy/EB. **H2**, on the other hand, displayed poor selectivity and even ambivalence in certain instances, and would not be a candidate for such purifications.

3.4 SCXRD analyses

Table 3 summarizes all the relevant crystallographic data for the five complexes produced in this work. **H1**·*o*-Xy crystallized in the monoclinic crystal system and space group $P2_1/c$, while all four complexes of **H2** were solved in the triclinic crystal

Table 3 Relevant crystallographic data for the complexes of **H1** and **H2** with the xylenes and ethylbenzene

	H1·*o*-Xy	**H2**·*o*-Xy	**H2**·*m*-Xy	**H2**·*p*-Xy	**H2**·EB
Chemical formula	$C_{29}H_{24}O{\cdot}C_8H_{10}$	$C_{29}H_{22}Cl_2O{\cdot}C_8H_{10}$	$C_{29}H_{22}Cl_2O{\cdot}C_8H_{10}$	$C_{29}H_{22}Cl_2O{\cdot}C_8H_{10}$	$C_{29}H_{22}Cl_2O{\cdot}C_8H_{10}$
Formula weight	494.64	563.52	563.52	563.52	563.52
Crystal system	Monoclinic	Triclinic	Triclinic	Triclinic	Triclinic
Space group	$P2_1/c$	$P\bar{1}$	$P\bar{1}$	$P\bar{1}$	$P\bar{1}$
μ (Mo-Kα)/mm^{-1}	0.069	0.240	0.241	0.248	0.248
a/Å	9.8100(6)	9.760(4)	9.830(3)	10.3172(19)	9.8151(4)
b/Å	30.3835(16)	10.850(4)	10.658(3)	12.742(2)	10.9036(5)
c/Å	9.5691(6)	15.146(5)	15.343(4)	13.082(2)	14.5415(6)
Alpha/°	90	98.370(17)	96.197(10)	67.795(9)	94.486(2)
Beta/°	104.685(2)	96.251(17)	96.104(11)	71.424(8)	97.7538(19)
Gamma/°	90	103.375(17)	105.604(11)	72.877(9)	104.6528(19)
V/Å^3	2759.0(3)	1526.8(10)	1523.7(8)	1479.3(4)	1481.57(11)
Z	4	2	2	2	2
F(000)	1056	592	592	592	592
Temp./K	200	296	296	296	200
Restraints	0	124	126	0	0
Nref	6848	7515	7345	7386	7364
Npar	347	369	416	364	363
R	0.0530	0.0527	0.0462	0.0459	0.0429
wR_2	0.1309	0.1610	0.1544	0.1341	0.1195
S	1.04	1.05	1.07	1.02	1.03
θ min–max/°	2.1, 28.3	2.0, 28.5	2.0, 28.4	1.7, 28.5	1.9, 28.3
Tot. data	83 453	21 529	59 921	61 561	53 899
Unique data	6848	7515	7345	7386	7364
Observed data [$I > 2.0$ sigma(I)]	5197	4946	4675	5264	5923
R_{int}	0.028	0.027	0.054	0.041	0.019
Completeness	1.000	0.994	0.997	0.994	1.000
Min. resd. dens. (e Å^{-3})	−0.25	−0.46	−0.43	−0.45	−0.40
Max. resd. dens. (e Å^{-3})	0.24	0.47	0.36	0.36	0.32

system and space group $P\bar{1}$. The host packing in three of these **H2** inclusion compounds was isostructural, namely in **H2**·*o*-Xy, **H2**·*m*-Xy and **H2**·EB, while this packing was unique in **H2**·*p*-Xy. Only two guest components displayed disorder in these crystals: *o*-Xy in **H2** required a number of constraints and restraints in order to model it, and *m*-Xy, also in **H2**, experienced disorder over two positions.

Illustrative host···guest unit cell and packing diagrams are provided in Fig. 1a–c (left) which were prepared using Mercury software[27] (here, the **H2**·*o*-Xy illustration represents also **H2**·*m*-Xy and **H2**·EB, the host packing in each being isostructural). Also given here are the void diagrams (right, yellow) which demonstrate the nature of the guest accommodation, and which were obtained by removing the guests from the packing calculations. All guests appeared to occupy constricted channels in the host crystals.

Surprisingly, no classical host···host intermolecular H-bonding could be identified in any of these complexes, but two or three non-classical interactions of this type were present in each one, involving either the host protons of the free aromatic ring systems or the roof methylene protons and the oxygen atom of the hydroxyl functionality. These were all intramolecular in nature, maintaining the host molecular geometry, and measured between 2.31 and 2.56 Å (H···A) with associated angles between 102 and 106°. Fig. 2a and b are illustrations depicting the two non-classical H-bonding

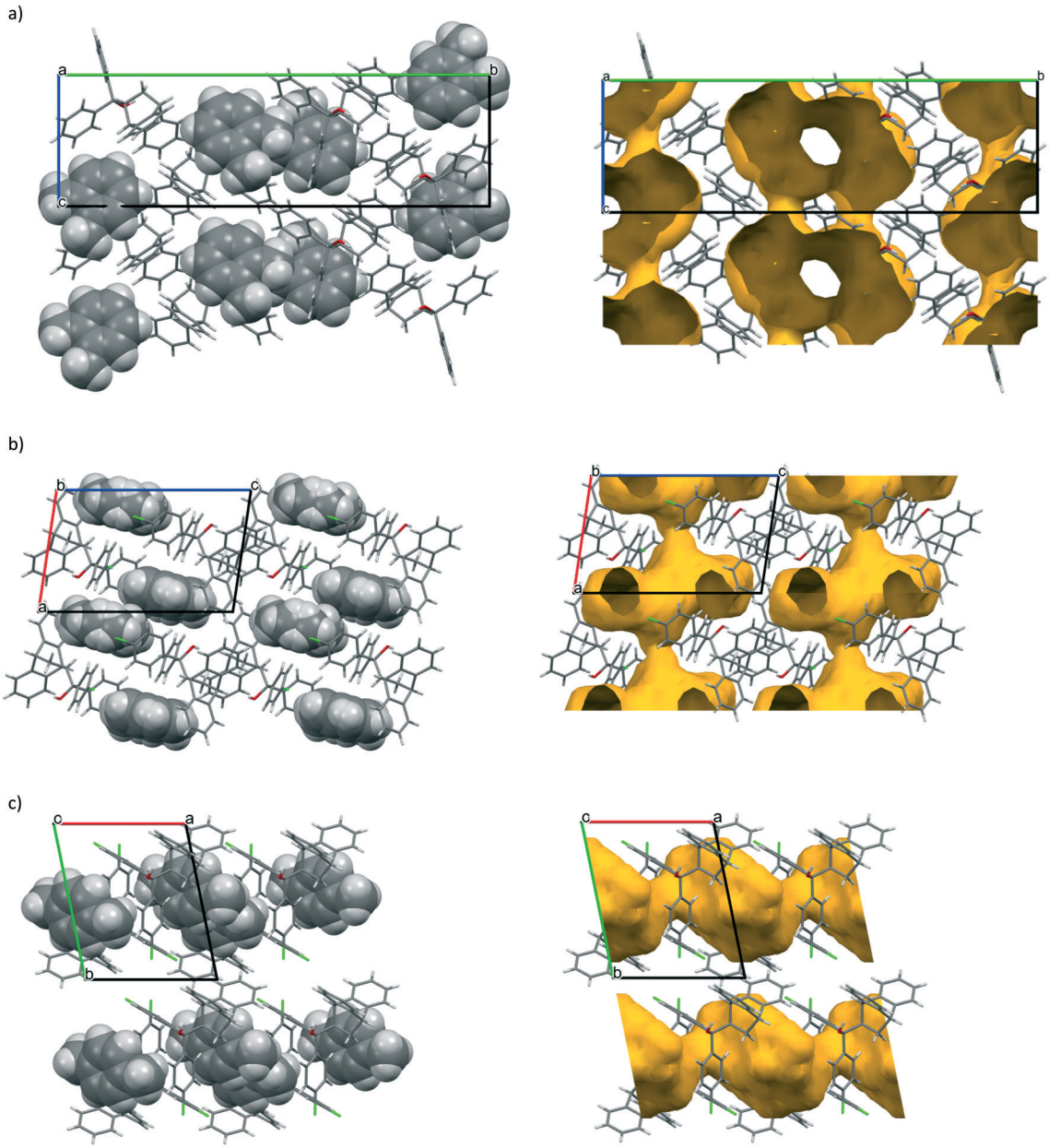

Fig. 1 Unit cell and host–guest packing diagrams (left) and voids (right, yellow) in a) **H1**·*o*-Xy, along [100], b) **H2**·*o*-Xy (also representing **H2**·*m*-Xy and **H2**·EB), along [010], and c) **H2**·*p*-Xy, along [001].

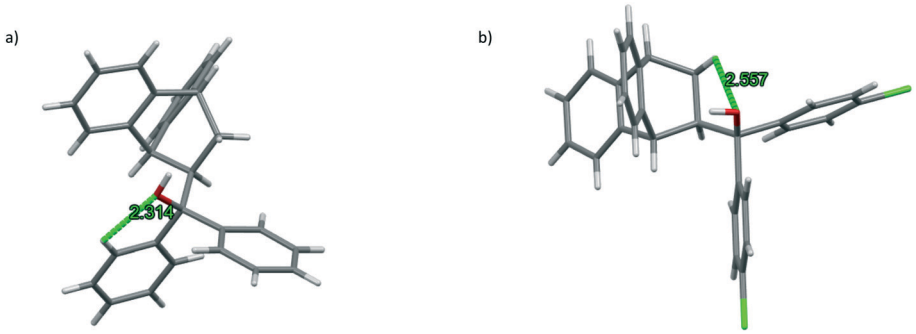

Fig. 2 Intramolecular host···host non-classical hydrogen bonding interactions maintaining the host molecular geometry of the a) free Ar–H···O (in **H1**·*o*-Xy) and b) roof HC–H···O (in **H2**·*o*-Xy) type; guest molecules have been removed for clarity.

interactions employing **H1**·*o*-Xy and **H2**·*o*-Xy as representative examples, respectively, where guest molecules have been omitted for clarity.

Furthermore, all complexes of **H2** presented intermolecular host···host π···π and intramolecular host···host O–H···π interactions that assisted in both packing the host molecules in three dimensions and maintaining their geometry, and these are illustrated in Fig. 3a and b using **H2**·*p*-Xy (3.64 Å, with a slippage of 1.02 Å) and **H2**·EB (H···Cg, 2.58 Å, with an associated angle of 156°) as examples, respectively (again, the guest molecules have been removed). Note that these interaction types were not present in **H1**·*o*-Xy and, in the latter instance, the bond between the host hydrogen and oxygen atoms was oriented in a significantly less perpendicular fashion relative to the adjacent fused aromatic ring of **H1**, ensuring the absence of any meaningful intramolecular host···host O–H···π interactions. This is illustrated in Fig. 3c where the red areas are the calculated planes of the relevant fused aromatic ring and the C–O–H group.

However, an intermolecular O–H···π interaction was identified in **H1**·*o*-Xy where the hydroxyl group of one host molecule interacts favourably with an aromatic ring double bond on a neighbouring host molecule. This interaction measured 2.75 Å which is significantly less than the sum of the van der Waals radii (2.90 Å).

Any other π···π interactions in these complexes were not significant, and guest retention was not reliant upon this interaction type.

Both host and guest species in **H1**·*o*-Xy experienced C–H···π interactions involving the host free aromatic protons and the guest centroid (2.78 and 2.97 Å, 151 and 136°) (H···π, C–H···π) as well as the guest aromatic and methyl protons and the host aromatic centres of gravity (2.88 and 2.96 Å, 153 and 150°). These were further accompanied by (host)ArC–H···C–C(guest) (2.87 Å, 142°) and (guest)C–H···H–C(host) (2.36 Å, 174°) stabilizing contacts. All of the aforementioned

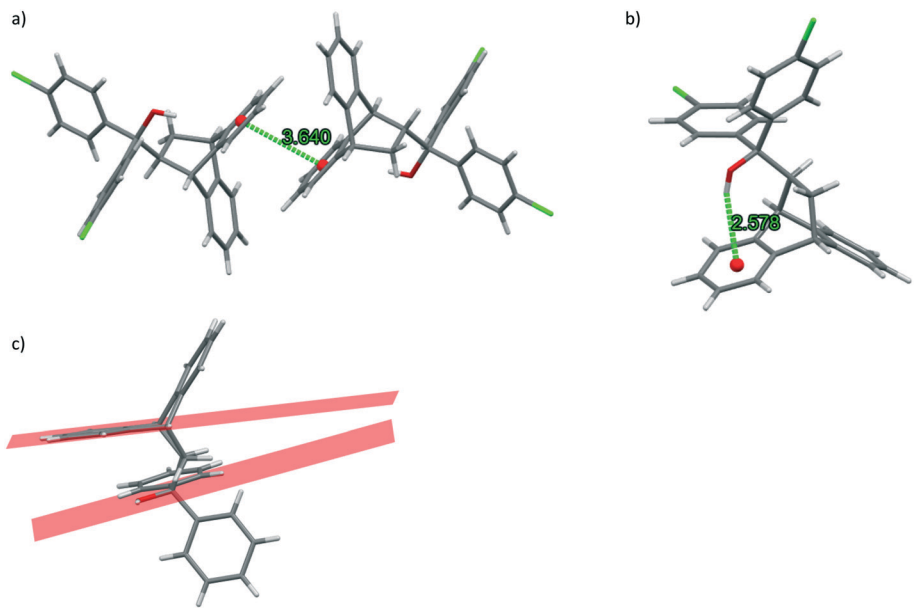

Fig. 3 Host···host a) intermolecular π···π (in **H2**·*p*-Xy) and b) intramolecular OH···π (in **H2**·EB) interactions; c) the calculated planes (red) of the adjacent fused aromatic ring system and the C–O–H group of **H1** in **H1**·*o*-Xy; guest molecules are not shown here.

Table 4 Host···guest interactions present in the complexes with **H2**[a]

Interaction type	**H2**·*o*-Xy	**H2**·*m*-Xy	**H2**·*p*-Xy	**H2**·EB
(Host)C–H···π(guest)	2.86 Å, 139° 2.83 Å, 150°	2.94 Å, 142° 2.78 Å, 150° 2.82 Å, 152°	2.74 Å, 154°	2.91 Å, 152°
(Guest)C–H···π(host)	2.91 Å, 150° 2.95 Å, 131° 2.54 Å, 157°	2.83 Å, 166° 2.93 Å, 125° 2.92 Å, 140°	2.95 Å, 154°	2.97 Å, 143°
(Guest)C–H···C–C(host)	2.77 Å, 151°, < 2.24 Å, 132°, ≪	2.84 Å, 136°, < 2.81 Å, 150°, < 2.80 Å, 151°, <	None	None
(Host)C–C···H–C(guest)	2.86 Å, 153°, <	None	None	None
(Host)C–H···H–C(guest)	1.96 Å, 142°, ≪	None	None	None
(Host)C–H···C–C(guest)	2.85 Å, 153°, <	None	None	2.89 Å, 136°, <

[a] < denotes contacts less than the sum of the van der Waals radii and ≪ contacts less than this sum minus 0.2 Å.

interactions were thus responsible for the retention of the *o*-Xy guest within the **H1** crystals.

The host···guest interactions that were identified in the four complexes with **H2** are summarized in Table 4 for ease of comparison.

Both the preferred *o*-Xy guest as well as *m*-Xy experienced a large number of stabilizing host/guest···guest/host interactions (Table 4) but only *o*-Xy was involved in contacts that measured significantly less than the sum of the van der Waals radii of the atoms involved. Two such close interactions were observed, namely of the (guest)C–H···C–C(host) (2.24 Å, 132°) and (host)C–H···H–C(guest) (1.96 Å, 142°) types. These interactions are significant and certainly contribute towards the affinity of **H2** for *o*-Xy. *p*-Xy and EB, on the other hand, were involved in only very few interactions with this host compound.

In order to further investigate the affinity of **H2** for *o*-Xy, we considered Hirshfeld surface analyses and their associated two-dimensional fingerprint plots. These three-dimensional surfaces are used to describe the immediate surroundings of molecules and to explore, quantitatively, the various host···guest and guest···host interactions.[28] Here, we generated these surfaces around the guest molecules using Crystal Explorer 17 software,[29] and these data were then

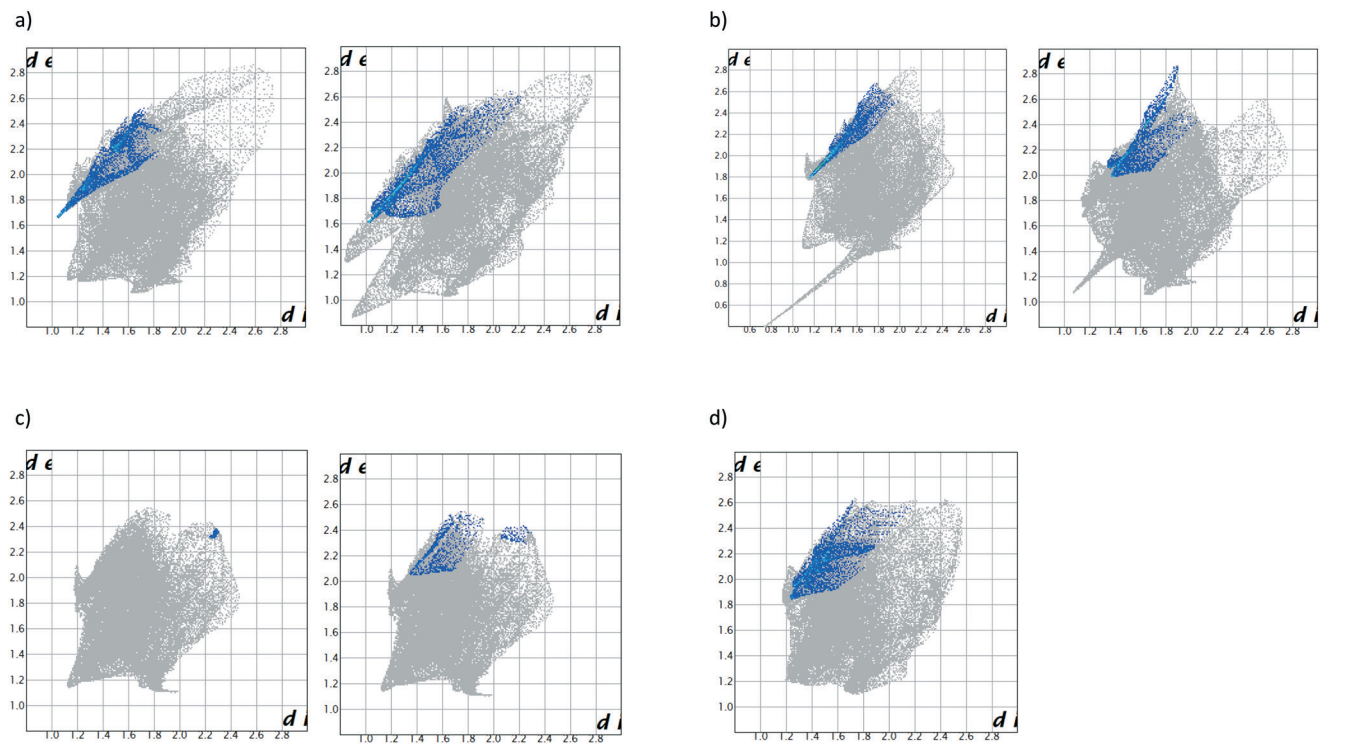

Fig. 4 Fingerprint plots showing host chlorine atom interactions with a) guest hydrogen atoms in **H2**·*o*-Xy (one disordered component, left, and the other, right), b) guest hydrogen atoms in **H2**·*m*-Xy (one disordered component, left, and the other, right), c) guest carbon atoms (0.2%, left) and guest hydrogen atoms (2.1%, right) in **H2**·*p*-Xy, and d) guest hydrogen atoms in **H2**·EB.

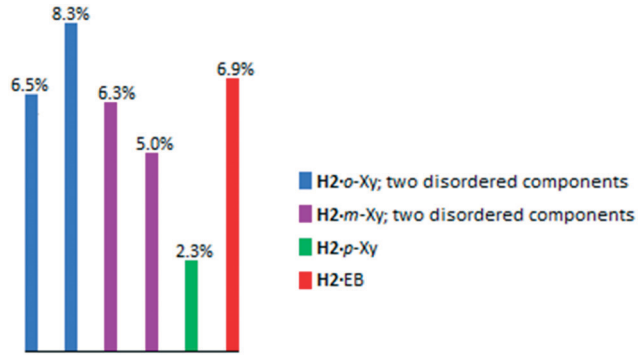

Fig. 5 A quantitative depiction of the percentage of host chlorine atom interactions with any guest atoms (more usually hydrogen).

translated into the fingerprint plots. In Fig. 4a–d, d_e and d_i are the distances to the nearest atom outside and inside the guest surface, respectively (note that we considered the two disordered guest components in **H2**·*o*-Xy and **H2**·*m*-Xy separately). In particular, we analysed the interactions of the chlorine atoms of the host compound with the guest species, and these are depicted as the blue highlights in these figures. In all but one case, the host chlorine atoms interacted only with guest hydrogen atoms [the exception is (host)Cl···C(guest) interactions in **H2**·*p*-Xy, but this contribution was only small (0.2%) compared with the (host)Cl···H(guest) interactions (2.1%)].

In order to visually describe these observations, a bar graph was prepared (Fig. 5) and, interestingly, overall, the preferred guest species of **H2** (*o*-Xy) was involved in a greater percentage of stabilizing interactions with the chlorine atoms of the host molecule (6.5, 8.3%) than the other guest molecules. This observation may further explain this host compound's selection of *o*-Xy. Additionally, and as alluded to before, the host packing in **H2**·*p*-Xy was unique compared with the other three complexes (which displayed isostructural host packing), and this is evident in Fig. 5: the percentage of host chlorine atom interactions with *p*-Xy was significantly lower (2.3%) than in the other complexes (5.0–8.3%), and this may well be as a result of the different packing in this crystal.

3.5 Thermal analysis

The thermal data, in the form of overlaid differential scanning calorimetric (DSC), thermogravimetric (TG), and its derivative (DTG), traces obtained after heating each sample at a rate of 10 °C min^{-1} from approximately 40 to 400 °C, are provided in Fig. S3a–e in the ESI.† The onset temperatures for the guest release process (T_{on}), estimated from the DTG traces, is a measure of the relative thermal stability of each complex, and these data are summarized in Table 5 together with measured and expected mass losses upon complete guest removal from the host crystals.

Guest removal from **H1**·*o*-Xy occurred in two broad steps, initiating at 64.0 °C, with the host melting endotherm peaking at 189.4 °C prior to which all of the guest compound had escaped (Fig. S3a,† Table 5). Prof. Weber reported that pure **H1** melted between 191 and 192 °C.[17] On the other hand, the lower melting host **H2** (124–125 °C (ref. 17)) experienced concomitant guest release and host melt processes. Furthermore, all of the guests of **H2**, with the exception of EB, were released in a single step (Fig. S3b–e†); the complex containing EB was not stable at room temperature and was released in two steps, the first of these occurring right from the outset of the experiment, and hence accurate T_{on} and mass loss measurements could not be made in this particular case. Notably, this guest was often discriminated against in the competition experiments (Table 2), and the poor thermal stability of this complex may explain this observation. We also observed that the preference of **H2** for *o*-Xy when mixed with any other guest could not be explained using these thermal data: the most stable complex was that with *m*-Xy (T_{on} 120.0 °C), while the complex containing *o*-Xy appeared less stable (108.8 °C). Also notable is that measured and expected mass losses were in similar to lower-than-expected ranges.

Table 5 T_{on} measurements and measured and expected mass losses for the complexes of **H1** and **H2**

Complex	T_{on}[a]/°C	Measured mass loss/%	Expected mass loss/%
H1·*o*-Xy	64.0	18.3	21.5
H2·*o*-Xy	108.8	16.0	18.8
H2·*m*-Xy	120.0	16.8	18.8
H2·*p*-Xy	100.7	15.6	18.8
H2·EB	[b]	[b]	18.8

[a] T_{on} is the onset temperature for the guest release process and is determined from the DTG trace. [b] The complex was unstable at room temperature.

4. Conclusion

α,α-Diphenyl-9,10-dihydro-9,10-ethanoanthracene-11-methanol **H1** and α,α-bis(*p*-chlorophenyl)-9,10-dihydro-9,10-ethanoanthracene-11-methanol **H2** were recrystallized from each of the xylenes (*o*-Xy, *m*-Xy and *p*-Xy) and ethylbenzene (EB) to assess their host selectivity towards these solvents. **H1** only formed a complex with *o*-Xy in these conditions while **H2** enclathrated each one. Mixed guest solvent competition experiments showed that **H1** possessed an enhanced selectivity for *o*-Xy when the other guest was *m*-Xy, *p*-Xy or EB (84.5–93.7%), while no crystals could be recovered from the remaining binary, ternary and quaternary guest combinations. The selectivity of **H2** in such competition experiments, on the other hand, was, however, only extremely ordinary (40.1–74.6 °C). This work has demonstrated that **H1** may be employed to purify *o*-Xy/*m*-Xy, *o*-Xy/*p*-Xy and *o*-Xy/EB binary mixtures when these guests are present in specified concentrations. **H2** does not have the ability to serve in this manner. SCXRD analyses showed that the preferred guest of **H2**, *o*-Xy, was the only one to experience very short contacts with the host molecule, thus

explaining the preference of **H2** for this guest. Additionally, data from Hirshfeld surface analyses concurred, and *o*-Xy experienced a greater percentage of stabilizing interactions with the chlorine atoms of the host compound. However, thermal analyses were less useful in explaining the selectivity order of **H2** for these aromatic guest solvents.

Author contributions

Benita Barton: conceptualization; funding acquisition; methodology; project administration; resources; supervision; visualization; writing – original draft. Brandon Barnardo: investigation; methodology; validation. Eric C. Hosten: data curation; formal analysis.

Conflicts of interest

There are no conflicts of interest to declare.

Acknowledgements

Financial support is acknowledged from the Nelson Mandela University and the National Research Foundation (NRF) of South Africa.

References

1 W. Qia, X. Wanga, Z. Liu, K. Liu, Y. Long, W. Zhi, C. Ma, Y. Yan and H. Huang, Visual recognition of *ortho*-xylene based on its host-guest crystalline self-assembly with α-cyclodextrin, *J. Colloid Interface Sci.*, 2021, **597**, 325–333.

2 S. H. Kim, J. H. Park, E. M. Go, W.-S. Kim and S. K. Kwak, Separation principle of xylene isomers and ethylbenzene with hydrogen-bonded host frameworks via first-principles calculation, *J. Ind. Eng. Chem.*, 2020, **85**, 276–281.

3 M. M. Wicht, L. M. Obiang and L. R. Nassimbeni, Cobalt Werner hosts with nicotinamides: characterisation of mixed ligand complexes and their selectivity towards *ortho*-xylene, *Polyhedron*, 2021, **202**, 115202.

4 M. Lusi and L. J. Barbour, Solid-vapour sorption of xylenes: prioritized selectivity as a means of separating all three isomers using a single substrate, *Angew. Chem., Int. Ed.*, 2012, **51**, 3928–3931.

5 C. Pudack, M. Stepanski and P. Fässler, PET recycling – contributions of crystallization to sustainability, *Chem. Ing. Tech.*, 2020, **92**, 452–458.

6 B. Barton, E. C. Hosten and P. L. Pohl, Discrimination between *o*-xylene, *m*-xylene, *p*-xylene and ethylbenzene by host compound (R,R)-(−)-2,3-dimethoxy-1,1,4,4-tetraphenylbutane-1,4-diol, *Tetrahedron*, 2016, **72**, 8099–8105.

7 B. Barton, L. de Jager and E. C. Hosten, Minor modifications afford improved host selectivities in xanthenyl-type host systems, *CrystEngComm*, 2019, **21**, 3000–3013.

8 B. Barton, M. R. Caira, L. de Jager and E. C. Hosten, *N*,*N*′-Bis(9-phenyl-9-thioxanthenyl)ethylenediamine: highly selective host behavior in the presence of xylene and ethylbenzene guest mixtures, *Cryst. Growth Des.*, 2017, **17**, 6660–6667.

9 B. Barton, D. V. Jooste and E. C. Hosten, Synthesis and assessment of compounds *trans*-*N*,*N*′-bis(9-phenyl-9-xanthenyl)cyclohexane-1,4-diamine and *trans*-*N*,*N*′-bis(9-phenyl-9-thioxanthenyl)cyclohexane-1,4-diamine as hosts for potential xylene and ethylbenzene guests, *J. Inclusion Phenom. Macrocyclic Chem.*, 2019, **93**, 333–346.

10 B. Barton, U. Senekal and E. C. Hosten, Compounds *N*,*N*′-bis(9-cyclohexyl-9-xanthenyl)ethylenediamine and its thio derivative, *N*,*N*′-bis(9-cyclohexyl-9-thioxanthenyl)ethylenediamine, as potential hosts in the presence of xylenes and ethylbenzene: conformational analyses and molecular modelling considerations, *Tetrahedron*, 2019, **75**, 3399–3412.

11 B. Barton, D. V. Jooste and E. C. Hosten, Behaviour of host compounds 1,2-DAX and 1,2-DAT in the presence of mixed xylene and ethylbenzene guest solvents, and comparisons with their 1,4 host derivatives, *J. Inclusion Phenom. Macrocyclic Chem.*, 2021, **100**, 155–167.

12 L. R. Nassimbeni, N. B. Báthori, L. D. Patel, H. Su and E. Weber, Separation of xylenes by enclathration, *Chem. Commun.*, 2015, **51**, 3627–3629.

13 K. Jie, M. Liu, Y. Zhou, M. A. Little, A. Pulido, S. Y. Chong, A. Stephenson, A. R. Hughes, F. Sakakibara, T. Ogoshi, G. M. Day, F. Huang and A. I. Cooper, Near-ideal xylene selectivity in adaptive molecular pillar[n]arene crystals, *J. Am. Chem. Soc.*, 2018, **140**, 6921–6930.

14 Z. Zhang, S. B. Peh, C. Kang, K. Chai and D. Zhao, Metal-organic frameworks for C6–C8 hydrocarbon separations, *EnergyChem*, 2021, **3**, 100057.

15 A. Altaf, N. Baig, M. Sohail, M. Sher, A. Ul-Hamid and M. Altaf, Covalent organic frameworks: Advances in synthesis and applications, *Mater. Today Commun.*, 2021, **28**, 102612.

16 Q. Shi, J. C. Gonçalves, A. F. P. Ferreira and A. E. Rodrigues, A review of advances in production and separation of xylene isomers, *Chem. Eng. Process.*, 2021, **169**, 108603.

17 E. Weber, T. Hens, O. Gallardo and I. Csöregh, Roof-shaped hydroxy hosts: synthesis, complex formation and X-ray crystal structures of inclusion compounds with EtOH, nitroethane and benzene, *J. Chem. Soc., Perkin Trans. 2*, 1996, 737–745.

18 B. Barton, U. Senekal and E. C. Hosten, Comparing the host behaviour of roof-shaped compounds *trans*-9,10-dihydro-9,10-ethanoanthracene-11,12-dicarboxylic acid and its dimethyl ester in the presence of mixtures of xylene and ethylbenzene guests, *CrystEngComm*, 2021, **23**, 4560–4572.

19 B. Barton, U. Senekal and E. C. Hosten, *trans*-α,α,α′,α′-Tetraphenyl-9,10-dihydro-9,10-ethanoanthracene-11,12-dimethanol and its tetra(*p*-chlorophenyl) derivative: roof-shaped host compounds for the purification of aromatic C_8H_{10} isomeric guest mixtures, *J. Inclusion Phenom. Macrocyclic Chem.*, 2021, DOI: 10.1007/s10847-021-01102-5, submitted.

20 O. Helmle, I. Csöregh, E. Weber and T. Hens, Supramolecular crystalline complexes involving bulky hydroxy hosts: X-ray

structure analysis of inclusion compounds with acetone and toluene, *J. Phys. Org. Chem.*, 1997, **10**, 76–84.

21 I. Csöregh, E. Weber and T. Hens, The role of chloro substituents in solid inclusion formation. Crystal structures formed by a bulky hydroxy host with ethyl acetate (2:1) and cyclohexylamine (1:2) as guest, *Supramol. Chem.*, 1998, **10**, 133–142.

22 N. M. Sykes, H. Su, E. Weber, S. A. Bourne and L. R. Nassimbeni, Selective enclathration of methyl- and dimethylpiperidines by fluorenol hosts, *Cryst. Growth Des.*, 2017, **17**, 819–826.

23 A. Bruker, *APEX2, SADABS and SAINT*, Bruker AXS, Madison, 2010.

24 G. M. Sheldrick, SHELXT–Integrated space-group and crystal-structure determination, *Acta Crystallogr., Sect. A: Found. Adv.*, 2015, **71**, 3–8.

25 G. M. Sheldrick, Crystal structure refinement with SHELXL, *Acta Crystallogr., Sect. C: Struct. Chem.*, 2015, **71**, 3–8.

26 C. B. Hübschle, G. M. Sheldrick and B. Dittrich, ShelXle: a Qt graphical user interface for SHELXL, *J. Appl. Crystallogr.*, 2011, **44**, 1281–1284.

27 C. F. Macrae, I. Sovago, S. J. Cottrell, P. T. A. Galek, P. McCabe, E. Pidcock, M. Platings, G. P. Shields, J. S. Stevens, M. Towler and P. A. Wood, Mercury 4.0: from visualization to analysis, design and prediction, *J. Appl. Crystallogr.*, 2020, **53**, 226–235.

28 M. A. Spackman and D. Jayatilaka, Hirshfeld surface analysis, *CrystEngComm*, 2009, **11**, 19–32.

29 S. K. Wolff, D. J. Grimwood, J. J. McKinnon, D. Jayatilaka and M. A. Spackman, *Crystalexplorer 17.5*, University of Western Australia, Perth, 2007, hirshfeldsurface.net.

